Ultrawideband Radar Processing using Channel Information from Communication Hardware

Final Report

Bryan Westcott

Abstract— Channel information provided by impulse-radio ultrawideband communications hardware is used in radar applications requiring information about the surrounding physical environment. The methods presented are similar to sonar-based echolocation methods, but have the advantage that complex reflections can be analyzed. The localization and classification of multipath allows sonar-based map-building algorithms to be applied. Novel solutions are presented for reflection classification and map building for multi-user, multi-antenna, and single-antenna hardware.

EMERGING ultrawideband (UWB) technology potentially offers not only hundred-megabit-per-second data rates for wireless communications, but also sub-centimeter resolution radar applications [2]. The short pulse duration of impulse-radio implementations allows most of the dominant multipath reflections in the environment to be individually resolved [1] and this multipath energy may be collected with a Rake receiver, which is common with spread-spectrum communications. Channel estimation is crucial to the performance of wideband receivers, but also provides information about the local environment. This paper explores the options for mapping the local physical environment from channel information already obtained by communications hardware.

Location-based services, such as emergency-911, are already proving popular in the cellular industry [3], but do not provide high-precision localization. GPS is extremely popular for navigation, but is also limited in accuracy and does not work well indoors [4]. The algorithms presented could complement existing technologies, particularly useful for indoor and urban navigation. The algorithms would be useful for navigating known environments, such as guiding a person through an unfamiliar building. The algorithms could also be useful for the exploration of unknown environments by robots, dangerous environments by emergency response workers, and hostile environments such as military teams in urban conflicts. This would only require communication hardware, which may already be in use to connect to local hotspots or other users in a team. In addition, location-based security is a great potential application to prevent wireless networks from being accessed outside of a building [5]. Also, future "augmented reality" applications would require extremely precise location measurements.

The methods presented in this report are similar to sonar-based 'echolocation' algorithms. In these algorithms the reflection time, or time-of-flight (TOF) of wideband ultrasound pulses provide information about the local environment. Both ultrasound and ultrawideband have similar specular propagation [1] where large surfaces have mirror-like reflection, right-angle corners reflect back to all directions, and edges diffract to all directions. If these features can be identified and localized in UWB implementations, the sonar-based map-building algorithms may be used. Sonar implementations typically use directional arrays that measure not only distance but direction to all reflections. This may seem to place omnidirectional communication antennas at a disadvantage; however, directional arrays can only measure reflections from normal surfaces (where the normal projection of the antenna location onto a finite-area surface exists). If done correctly and efficiently, electromagnetic echolocation can provide more complex mapping because signals reflecting off of multiple surfaces and arriving from all directions can be analyzed, and 'hidden' non-normal surfaces can be located.

One relevant sonar-based method is a relocation algorithm by Lim and Leonard [6]. It is one of the few methods based on range information alone, but requires a known map of the local environment, which this paper is trying to produce. The goal of

this method is to find the location on the map that best fits the range data obtained, and this method could easily be extended to any of the hardware configurations presented in this paper. A method designed specifically for map-building is presented by Kuc and Siegel [7]. After locating and then classifying the reflections as corners, edges or walls, a map is constructed with known shadowed regions. Finally, a method by Guivant and Nebot [8] uses an extended Kalman filter to estimate and update the current estimate of position, while simultaneously building and maintaining a map of the local environment. This method is particularly useful as some of the methods in this paper may present multiple solutions. Also, while the methods presented may be complex, they would only have to be performed once if a Kalman filter is used. Any of these methods may be used, but it first requires that reflection location and classification be performed with a single antenna, and with communications hardware.

The specular propagation of both methods allows a channel to be estimated with simple ray tracing techniques. A three dimensional room with moderate complexity is represented in two dimensions in simulation. The local and distributed users may be randomly placed, and the peaks in the expected channel response will be determined by this ray tracing. Reflections, diffractions and double reflections are combined into one response, as in a real channel. Error can be simulated, but the receiver operation requires that it be less than the pulse width, which is three orders of magnitude less than typical room dimensions, making it insignificant. The general solutions were obtained using the symbolic math toolbox in Matlab.

Three novel algorithms using only the TOF of multipath reflections are presented; an extensive literature survey found no similar methods. The first assumes an environment with distributed sources of communication activity, with no cooperation necessary, where techniques such as successive interference cancellation are used to measure and then subtract the interference of other users to increase communication performance. This environment essentially provides distributed radar sources, which will be common if UWB becomes popular for networking and wire-replacement in electronics. The second technique assumes the use of two or more antennas, common with multiple-input multiple-output (MIMO) technologies and in wireless network cards providing spatial diversity, and essentially provides an antenna array. The final technique assumes the use of only one antenna and one communication receiver, and allows a two- or three-dimensional environment to be reconstructed from a simple one-dimensional impulse response. The derivation of each algorithm is presented, along with practical implementation issues and basic performance analyses.

I. Distributed Source Method

A. *First Implementation*

The first method presented assumes a spatially-distributed set of communication devices, possibly other wireless users or other devices such as wire-replacement devices that may become common for future multimedia devices. The distributed sources may

act independently of the local device, but it is assumed that the dominant multipath is decoded by the local user for interference cancellation algorithms. It is also assumed that the relative positions of the distributed users are known and that the offset between local clocks is accurately measured. Straightforward methods to obtain this information are proposed by the IEEE 802.15 TG4a WPAN Task Group [9] to be implemented in UWB communication chipsets.

This first method was inspired by a sonar-based algorithm by McKerrow [10] and works as follows: the dominant peaks in the channel response of the distributed user correspond to time-of-flight information. When combined with knowledge of the distributed user's position, a two-dimensional representation of the possible reflection points forms an ellipse. The user also measures the reflections of its own activity, and the possible single reflection points form a circle. When both reflections are on a common surface, the actual reflection locations form a line tangent to both conic sections. Solving both equations and their slopes through implicit differentiation [11] produces a maximum of two lines (see Figure 1), only one of which being the correct solution. (Figure 2 applies to the single-antenna case discussed in Section III, and is displayed here for comparison purposes.)

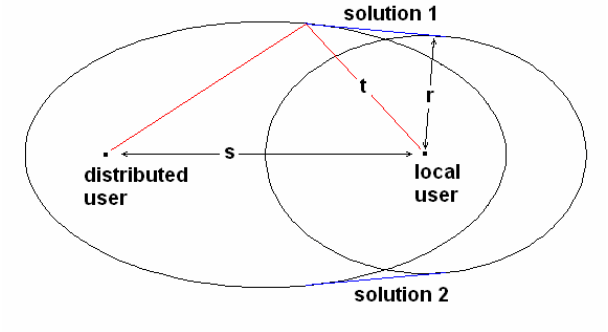

Figure 1, distributed source problem setup

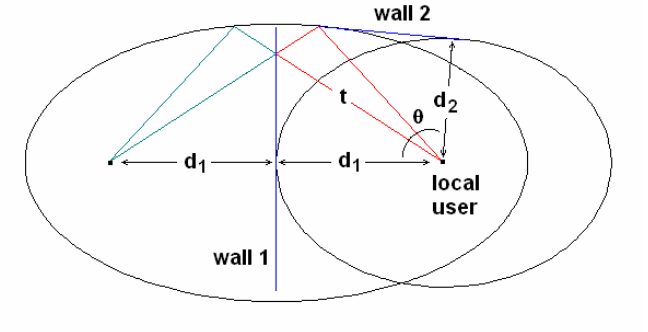

Figure 2, Single antenna problem setup

Using symbolic math with s representing the user separation, r representing the local user's self-reflection, and t representing the TOF, the solution is as follows:

$$x_1 = \frac{t^2(2r^2 - \frac{1}{2}t^2 + \frac{1}{2}s^2)}{s(t^2 - s^2 + 4r^2)}$$

$$y_1 = \frac{(16r^4t^2 - 3t^4s^2 - 16r^4s^2 - s^6 + 3s^4t^2 + t^6 + 8s^4r^2 - 8t^4r^2)}{2s(t^2 - s^2 + 4r^2)(-t^4 + 2t^2s^2 + 8t^2r^2 - s^4 + 8r^2s^2 - 16r^4)^{1/2}}$$

$$x_2 = \frac{(-t^2 - s^2 + 4r^2)}{4s}$$

$$y_2 = \frac{(-t^4 + 2t^2s^2 + 8t^2r^2 - s^4 + 8r^2s^2 - 16r^4)^{1/2}}{4s}$$

The position of a common diffracting corner corresponds to the intersections of the circle and ellipse; and the four solutions are as follows:

$$y_{1,2} = \pm \frac{(-4t^2r^2 - 4t^3r - t^4 + 4ts^2r + 2t^2s^2 - s^4 + 4r^2s^2)^{1/2}}{2s}$$

$$y_{3,4} = \pm \frac{(-4t^2r^2 + 4t^3r - t^4 - 4ts^2r + 2t^2s^2 - s^4 + 4r^2s^2)^{1/2}}{2s}$$

$$x_{1,2} = -\frac{2\mathrm{tr} + \mathrm{t}^2}{2\mathrm{s}}$$

$$x_{1,2} = +\frac{2\mathrm{tr} + \mathrm{t}^2}{2\mathrm{s}}$$

After these positions are calculated, the points must be rotated about the center of the circle to accurately reflect the relative positions of the users. Figure 3 shows all possible solutions for a sample environment, which is simulated with ray-tracing software. A wall is located by finding all collinear line segments, and a corner may be located by finding two or more collocated intersection solutions. A sample result is shown in Figure 4.

An extra benefit of this method is that the multiple collinear segments provide a reasonable estimate of the actual size of the wall. Efficient algorithms for rotation, collinearity tests and collocation tests are beyond the scope of this study.

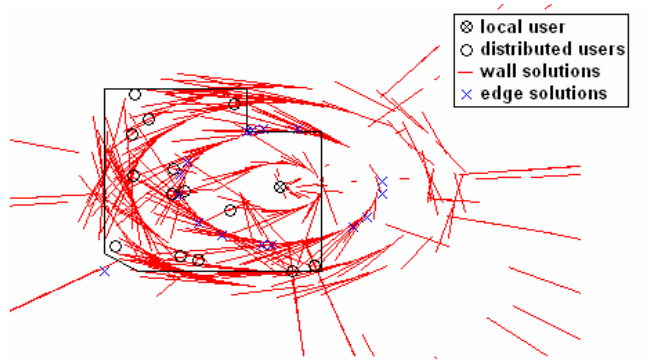

Figure 3, all possible wall solutions and edge solutions

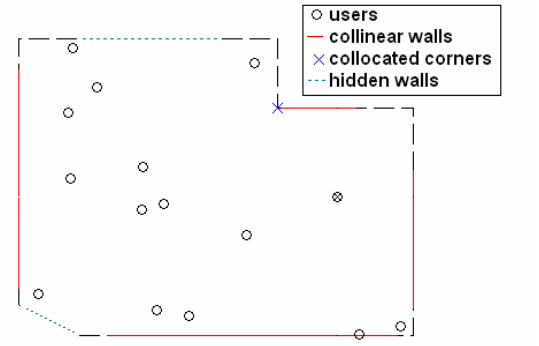

Figure 4, collinear wall solutions, collocated edge solutions, and 'hidden' wall solutions

As is obvious in Figure 3, some solutions are invalid (complex) and can be tested for before performing the calculations. No valid tangent or intersection solution will exist if the circle is completely inside the ellipse, or has a radius larger than the semi-minor axis, thus valid solutions satisfy:

$$t^2 - \tfrac{1}{4}s^2 < r^2 < (t + \tfrac{1}{2}s)^2$$

B. Second Implementation

It is not typically common in communications to measure the local user's self reflections, and these self reflections can only locate normal surfaces. To overcome these issues, this calculation may be performed by calculating the tangent between two ellipses from two distributed users. With this method the topmost and diagonal 'hidden' walls in Figure 4 could be located. The

disadvantage is that the solution is no longer linear with number of distributed users participating. The author was unable to obtain a symbolic solution due to time constraints; however, numeric and iterative methods may be possible as well.

It should be pointed out that this scenario is applicable to even the single antenna setup as it can be used in the refinement process. Once a few basic known walls are located, the antenna position can then be reflected about those walls to create a virtual distributed environment to find other 'hidden' features.

C. Performance

Since not all taps of the channel are resolved in practical SIC implementations, and since the number of users varies, the performance for these two variables is explored with simulation of randomized user positions. Figures 5a and 5b show the number of valid walls measured, compared to the maximum possible, and the number of false collinear hits, respectively. The first metric is roughly the same for increasing users or taps, however false hits slightly favor more users. The complexity of the calculation is also accounted for, linear in number of users and a square function of taps per user. If these quality measures are combined, the optimum number of users and taps is shown in Figure 5c.

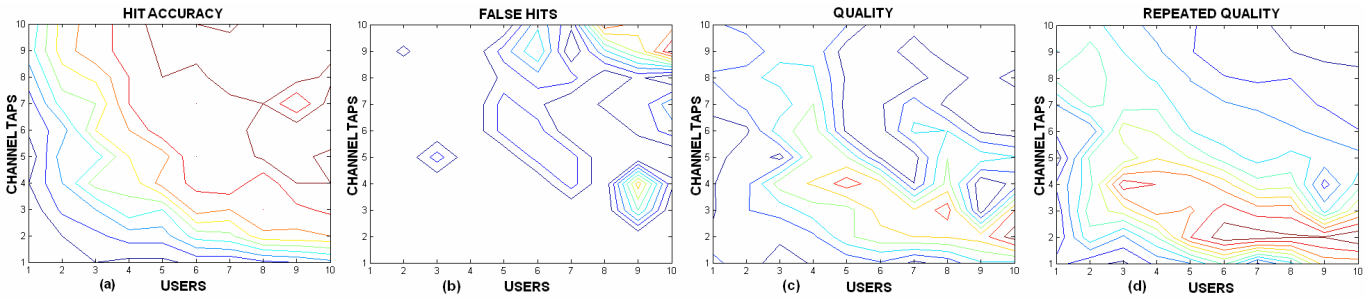

Figure 5, performance of distributed solution, (a) accuracy, (b) false hits, (c) performance, (d) repeated measurement performance

This shows a preference for more users, as it has the most spatial diversity for the least complexity. However, if temporal diversity is also used where it is assumed the dominant taps will vary, clearly the optimal quality begins to approach two to three users and taps in Figure 5d, which is significant because it has been shown that this is the upper limit on practical channel taps for wideband SIC [12].

II. Multiple Antenna Method

Multiple-antenna receivers allow for more accurate classification and localization of multipath. MIMO is becoming popular in wireless communications, and many network cards use two antennas to take advantage of spatial diversity. The following methods assume two antennas, but more could be combined. The self-reflections and cross-reflections will travel similar distances when reflecting off the same features, causing peaks to occur at very similar times on each channel. Peaks occurring within a given threshold of one another are then processed.

As shown in Figure 6, the two antennas can be analyzed by being reflected about a surface, and with some geometric manipulation common cases can be tested for. For a wall reflection, the combination of the two self-reflection times-of-flight t_{11} and t_{12}, the two cross-reflection times-of-flight t_{12} and $t_{21,}$ and the known antenna separation s will satisfy the following test and have the following wall locations (relative to the center of the array):

$$test_{wall} : t_{12}^2 = s^2 + t_{11}t_{22} \;\; and \;\; t_{12} = t_{21}$$
$$d_{refl} = \tfrac{1}{4}(t_{11} + t_{22})$$
$$\theta_{refl} = \pm \sin^{-1} \tfrac{1}{2s}(t_{22} - t_{11})$$

For the common case of a 90 degree corner, the reflection geometry is also shown in Figure 6. A corner may be identified by the following test and location:

$$test_{corner} : t_{11}^2 + t_{22}^2 = 2(t_{12}^2 + s^2) \;\; and \;\; t_{12} = t_{21}$$
$$x_{refl} = \tfrac{1}{2s}(-t_{22}^2 + t_{11}^2)$$
$$y_{refl} = \pm \tfrac{1}{2s}(-t_{22}^4 + 2t_{22}^2 t_{11}^2 - t_{11}^4 + 2s^2 t_{22}^2 + 2s^2 t_{11}^2 - s^4)^{1/2}$$

A diffracting edge reflection location is the same as the 90 degree corner, and the test is the following:

$$test_{edge} : t_{12} = t_{11} + t_{22} \;\; and \;\; t_{12} = t_{21}$$

While these methods will locate edges and corners, it is not possible to obtain the orientation of those features as an identical solution will be produced at an infinite number of orientations. However, an initial result is obtained and the orientation ambiguity is resolved with the context of other features (which may have the same ambiguity).

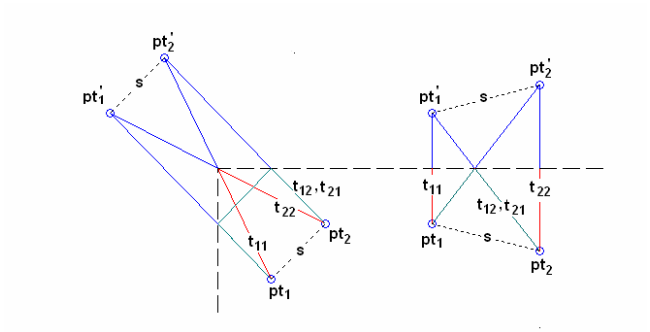

Figure 6, common MIMO reflections

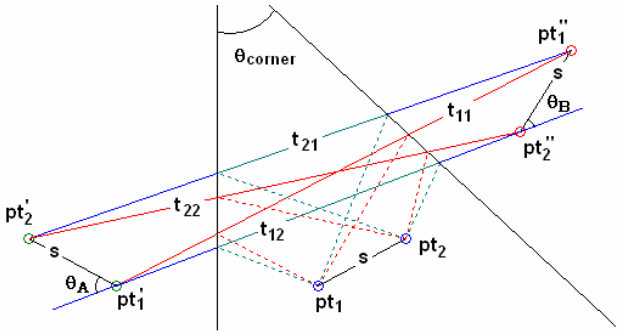

Figure 7, MIMO reflections from acute-angled corners

Finally, an acute-angled corner requires a more complex solution (see Figure 7) since the geometry has a great deal of possible variations. Acute-angled corners are virtually non-existent in common architecture; however in a closed room, one obtuse angle between adjacent walls must produce an acute angle between other non-adjacent walls. The reflected points will form a quadrilateral, but either t_{12} and t_{21} or t_{11} and dt_{22} will be the diagonals depending on the particular geometry. Accounting for this with some geometric manipulation, all possible valid reflection solutions satisfy one of the following two tests:

$$test_1 : \ 2\pi = angle_{1a} + angle_{1b} + angle_{2a} + angle_{2b}$$
$$test_2 : \ 0 = (angle_{1a} + angle_{1b}) - (angle_{2a} + angle_{2b})$$

$$angle_{1a} = \cos^{-1}((t_{22}^2 - t_{21}^2 - s^2)/(2t_{21}s))$$
$$angle_{1b} = \cos^{-1}((t_{11}^2 - t_{21}^2 - s^2)/(2t_{21}s))$$
$$angle_{2a} = \cos^{-1}((t_{11}^2 - t_{12}^2 - s^2)/(2t_{12}s))$$
$$angle_{2b} = \cos^{-1}((t_{22}^3 - t_{12}^2 - s^2)/(2t_{12}s))$$

If this test is satisfied a refinement process would be to reflect both antenna locations about all known walls, as a set of virtual distributed users. The double-ellipse tangent algorithm from Section I performed pair-wise between t_{11}, t_{12}, t_{21}, and t_{22} would necessarily present a solution if the previous test is satisfied. One other interesting result, however, is that the angle between walls of that corner can be calculated, using θ_A and θ_B as defined in Figure 7 as follows:

$$\theta_{corner} = \pi - \tfrac{1}{2}(\theta_A - \theta_B)$$

III. Single Antenna Solution

The final method explores the possibilities for a single antenna. The method used is as follows: two distance measurement to adjacent walls that meet at a corner are measured, when those measurements are combined with a double reflection off of both walls, the angle between the walls can be determined. The actual position of the walls cannot be determined, only the relative geometries.

The environment can then be reconstructed by combining all of this information into a single solution. This process also serves to classify which reflections are single reflections and which are double reflections. This classification can be further simplified by looking for parallel walls and right-angle corners, which are quite common. Once the single reflections are classified, the solution can be pieced together. The simplifications are as follows:

$$180^\circ : \ d_1 + d_2 = t$$
$$90^\circ : \ d_1^2 + d_2^2 = t^2$$

Finally, the solution for all other angles is obtained from a similar problem setup as in Section I. In this case a common technique in ray tracing is applied, whereby two reflections are calculated by reflecting the point about a known wall. This produces a virtual distributed source, mathematically. Thus the same solution can be used as in Figure 1 but only one side of the symmetric solution is used, and is shown in Figure 2. The wall locations are not known, so only the angle (as seen by the user) between wall reflections may be calculated. With d_1 and d_2 representing the distance to single reflections, and t representing a multipath reflection off of those two walls the angle may be calculated as follows:

$$angle = \frac{\pi}{2} - \tan^{-1}\left(\frac{(d_1^2 - t\text{^}2 + d_2^2)}{(-t^4 + 2t^2 d_1^2 + 2t_2 d_2^2 - d_1^4 + 2d_1^2 d_2^2 - d_2^4)^{1/2}} \right)$$

One important point is that a diffracting corner will act as a wall and must be identified as the previous equation is not valid. Due to time constraints an algebraic test could not be identified, however, it may be possible to threshold the dominant multipath, as a signal from a diffracting edge typically has much less power than single or double reflections.

Finally, once this basic map is calculated, refinements can be made by reflecting the local point about known walls and the single-ellipse distributed tangent algorithm presented in Section I can be performed. One issue with this method is that it produces two valid solutions, both having the same relative geometries, but one being a mirror image of the other. Tracking changes in the channel, corresponding to motion of the user, could help resolve this ambiguity.

IV. Conclusion

This work shows that relatively straightforward methods may be used to obtain two-dimensional or three-dimensional information about the local environment from one dimensional channel information. The methods also serve to differentiate multipath that is single reflections, double reflections or diffractions, a task that is quite a bit simpler with sonar algorithms. However, for a slow moving user, the initial work may be done once then updated with a Kalman filter. In addition, a Kalman filter allows the user to take advantage of temporal diversity since the channel estimation will not typically resolve every significant reflection at all times. The only modification these algorithms require is that channel information be provided from the communication hardware, if not already available.

References

[1] V. Hovinen, M. Hamalainen, and T. Patsi, "Ultra wideband indoor radio channel models: preliminary results," *IEEE Conf. on Ultrawideband Systems and Technologies*, 21-23 May 2002, pp. 75-79.

[2] L. Yang and G.B. Giannakis, "Ultra-wideband communications: an idea whose time has come," *IEEE Signal Processing Magazine,* vol. 21, no. 6, Nov. 2004, pp. 26-54.

[3] J. Blyler, "Location based services are positioned for growth," *Wireless Systems Design Newsletter*, Sept. 2003.

[4] F. van Diggelen, "Indoor GPS theory & implementation," *Proc. IEEE Position Location and Navigation Symp.*, 15-18 Apr. 2002, pp. 240-247.

[5] S. Garg, M. Kappes, and M. Mani, "Wireless access server for quality of service and location based access control in 802.11 networks," *Proc. IEEE Int. Symp. On Computers and Communications*, 1-4 Jul. 2002, pp. 819-824.

[6] J.H. Lim and J.J. Leonard, "Mobile robot relocation from echolocation constraints," *IEEE Trans. Pattern Analysis and Machine Intelligence,* vol. 22, no. 9, Sept. 2000, pp. 1035-1041.

[7] R. Kuc and M.W. Siegel, "Physically-Based Simulation Model for Acoustic sensor robot navigation," *IEEE Trans. Pattern Analysis and Machine Intelligence*, vol. 9, no. 6, Nov. 1987, pp. 766-778.

[8] J.E. Guivant and E.M. Nebot, "Optimization of the simultaneous localization and map-building algorithm for real-time implementation," *IEEE Trans. Robotics and Automation*, vol. 17, no. 3, Jun. 2001, pp. 242 – 257.

[9] "IEEE 802.15 WPAN Low Rate Alternative PHY Task Group 4a (TG4a)," http://www.ieee802.org/15/pub/TG4a.html, Feb. 2005.

[10] P.J. McKerrow, "Echolocation: From range to outline segments," *Proc. Int. Conf. on Intelligent Autonomous Systems*, pp. 239-247, Pittsburg, PA, 1993.

[11] "Tangent Common to Two Ellipses," http://mathforum.org/library/drmath/view/61599.html, Apr. 2005.

[12] J.G. Andrews and T. H. Meng, "Performance of MC-CDMA with Successive Interference Cancellation in a Multipath Fading Channel," *IEEE Trans. on Comm.,* May 2004, pp. 811-22.